České vysoké učení technické v Praze, Fakulta stavební

Czech Technical University in Prague, Faculty of Civil Engineering

doc. Ing. Petr Kabele, Ph.D.

Víceúrovňový přístup k popisu poškození ve vláknocementových kompozitech

Multiscale approach to characterization of damage in fiber reinforced cementitious composites

Summary

Quasi-brittle behavior of concrete in tension often causes formation of cracks, which may impair durability and sometimes even safety of concrete and reinforced concrete structures. One of possible ways to address this problem consists in reinforcing cementitious matrix with discontinuous fibers. In the present lecture, we focus on a class of so-called strain-hardening fiber reinforced cementitious composites (SHCC), which can, due to properly designed fiber reinforcement, sustain significant straining under increasing load in tension. The overall deformation is mostly attributed to formation and opening of a large number of distributed fine cracks bridged by fibers – a process called multiple cracking.

In the first part of the lecture, a multiscale framework for characterization and modeling of damage in SHCC materials is outlined. The proposed framework starts at the level of the composites' constituents and ends with the composites' performance when used in structural members. For each relevant length scale, dominant substructures and associated physical mechanisms of deformation and damage are identified and appropriate analytical/numerical models are presented. Attention is paid to ensuring proper interconnections among these models.

In the second part of the lecture, the effects of aggressive environment on mechanical performance of a selected SHCC are studied from the multiscale perspective. Consistent changes in relevant mechanical properties are observed across different scales. The effect of environmental exposure on macroscopic behavior (described by stiffness, strength, and hardening), is linked to changes of micromechanical parameters, such as matrix toughness and fiber-matrix bond.

In the conclusion, sustainable maintenance and construction of infrastructure with better durability and admissible environmental impact is identified as a prime area for the future use of SHCC materials. The presented research is one of stepping stones in this direction.

Souhrn

Kvazikřehké chování betonu v tahu je často příčinou vzniku trhlin, které mohou degradovat trvanlivost a někdy i bezpečnost betonových a železobetonových konstrukcí. Jeden z možných způsobů, jak čelit tomuto problému spočívá ve vyztužení cementové matrice přidáním rozptýlených vláken. V této přednášce se zaměříme na tzv. vláknocementové kompozity s tahovým zpevněním (strain-hardening fiber reinforced cementitious composites – SHCC), které mohou díky vhodně navrženému vláknovému vyztužení snášet poměrně velké deformace při zvyšujícím se tahovém namáhání. Jejich makroskopická deformace je pak z velké míry přisouzena vzniku a rozevírání velkého počtu rozptýlených jemných trhlinek přemostěných vlákny.

V první časti přednášky je v hlavních rysech nastíněn víceúrovňový rámec pro popis a modelování poškození v SHCC kompozitech. Navržený rámec začíná na úrovni složek kompozitu a končí na úrovni jeho chování při použití v konstrukčních prvcích. Pro každou relevantní úroveň rozlišení jsou identifikovány dominantní substruktury a s nimi spojené mechanismy přetváření a porušování a jsou uvedeny vhodné analytické/numerické modely. Pozornost je věnována tomu, aby bylo zajištěno náležité propojení mezi jednotlivými modely.

Druhá část přednášky je věnována víceúrovňovému pohledu na vliv agresivního prostředí na mechanické chování vybraného SHCC kompozitu. Konzistentní změny mechanických vlastností jsou pozorovány na různých úrovních rozlišení. Vliv prostředí na makroskopické chování (které je popsáno tuhostí, pevností a tahovým zpevněním) je uveden do souvislosti se změnami mikromechanických parametrů, jako je lomová houževnatost matrice a soudržnost vlákna s matricí.

V závěru je jako primární oblast budoucího využití SHCC kompozitů identifikována udržitelná údržba a výstavba infrastruktury s lepší trvanlivostí a přijatelným vlivem na životní prostředí. Výzkum prezentovaný v této přednášce tvoří jeden ze základů pro další rozvoj v tomto směru.

Klíčová slova

vláknocementové kompozity s tahovým zpevněním, mikro-/mezo-/makro-úroveň, mechanismy přetváření a porušování, analytické a numerické modelování, účinky agresivního prostředí

Keywords

strain-hardening fiber reinforced cementitious composites (SHCC), micro-/meso-/macro-scale, mechanisms of deformation and damage, analytical and numerical modeling, effects of aggressive environment

Contents

1. INTRODUCTION

1.1 Motivation and approaches behind the development of fiber reinforced cementitious composites

Concrete, in all its variety, has been the most widely used man-made construction material. In terms of mechanical behavior, one of concrete's few shortcomings consists in its relatively low strength and quasi-brittle behavior when exposed to tension. In reinforced concrete (R/C), steel bars are placed in structural members so as to take over tensile stresses. In spite of this, even R/C structures may exhibit cracks, which are usually induced by mechanical or environmental (e.g. thermal volume changes, shrinkage etc.) loads. Such cracks may compromise durability of the affected members since they pave the way for water and possibly other aggressive agents from environment to enter their inner structure. Subsequent reactions with steel reinforcement result in its volume expansion which leads to spalling of protective concrete cover and further deterioration of the structure. Quasi-brittleness of concrete may also impair structural safety, especially in structures exposed to accidental loads (e.g. during earthquake, impact or fire) or in complex structural details, where sufficient conventional reinforcement is technically difficult to carry out (e.g. beam-column joints, connections of R/C and steel elements).

In the history of concrete, two, at times interlinked, paths have been followed to eliminate the negative effects of cracking. One approach aims at eliminating cracks by increasing the strength of concrete. This can be achieved by using special admixtures, fine fillers, and lower water/cement ratio, which results in concrete with a denser microstructure. The fresh mix usually has good flowability and self-compacting properties. Such a concrete is less permeable to environmental agents, which improves its durability. On the other hand, the higher strength is paid for by increased brittleness when the material fails. For this class of materials, the term *high performance concrete* (HPC) has been widely accepted.

The other concept is based on addition of fibers into concrete mix, which, rather than affecting the strength, increase the energy that has to be exerted to form a traction-free crack – the fracture energy. Although various (most often natural) fibers used to be added to mortars in ancient times, the first and most widely used contemporary technology of this type is the *fiber reinforced concrete* (FRC). In this material, discontinuous fibers are directly added to a concrete mix. The amount of fibers is typically limited by the requirement of fresh mix workability to a maximum of about 2% by volume. As shown in Figure 1, the tensile behavior of ordinary FRC differs from that of concrete by the presence of a long "tail" in the tensile stress-strain curve,

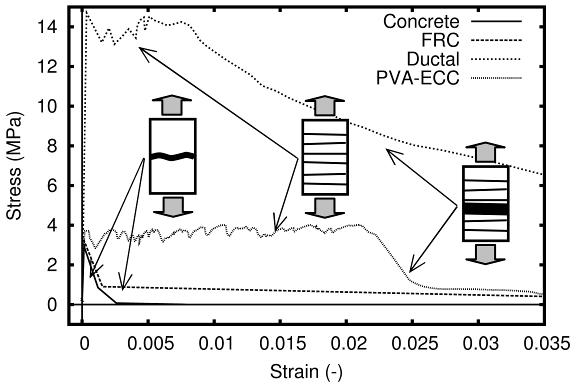

Figure 1 Typical uniaxial tensile stress-strain curves of quasi-brittle (concrete, FRC) and pseudo strain-hardening (Ductal, PVA-ECC) cementitious composites

which is attributed to a crack-bridging effect of fibers. Nevertheless in both materials, a single major crack forms and opens under uniaxial tension.

A qualitatively different fracture behavior under direct tension can be observed if the fiber bridging is sufficiently strong (more precise criteria are discussed later) to allow formation of subsequent fiber-bridged matrix cracks in a process called multiple cracking. The material then sustains increasing load with increasing overall deformation and its behavior is called pseudo strain-hardening or strain-hardening (see Fig 1). As a result, such a material can exhibit relatively large overall deformation while maintaining a macroscopic integrity. It may be also possible to control the crack width in such a range, that the cracks do not impair the material's durability. Reinhardt and Naaman [41], [45] introduced the term *high performance fiber reinforced cement composites* (HPFRCC) for this class of materials. Since the expression "high-performance" is rather general and it is used by different groups to emphasize different outstanding properties of materials that they developed (see e.g. the earlier mentioned HPC), RILEM technical committee 208-HFC [47] decided in 2005 to use a more descriptive term *strain-hardening fiber reinforced cementitious composites* (SHCC) instead. It has been found experimentally that some fiber reinforced cementitious composites may exhibit multiple cracking in bending, but not in direct tension. Relevant technical committee of Japan Concrete Institute (JCI) [12] therefore proposed a broader term *ductile fiber reinforced cementitious composites* (DFRCC), which encompasses both materials showing multiple cracking in bending and those in direct tension (HPFRCC or SHCC).

Pseudo strain-hardening and multiple cracking in cement-based composites can be achieved by various technologies. One technique is to employ continuous fibers or fabrics as reinforcement, as it is done, for example, in *textile reinforced concrete* (TRC) [2]. The use of fibers in the form of fabrics requires that a special production method is used, which makes TRC suitable only to a limited range of structural members (shells, sheets, pipes etc.). Other methods rely on the use of a high amount of discontinuous fibers (approximately 5 – 15% by volume). This also often results in the necessity to employ special production techniques. For example, in material called *slurry infiltrated fiber concrete* SIFCON [42], short steel fibers are first placed in a formwork and subsequently infiltrated by cement slurry. Materials commonly called *ultra high performance concretes* (UHPC) are based on dense cementitious matrices such as those of HPC, which are characteristic by strong but brittle behavior. To reduce brittleness, the mix is enhanced by addition of discontinuous fibers. Resulting composites, such as Ductal® [1], CARDIFRC® [9] or others retain high compressive and tensile strengths, but also exhibit some multiple cracking and moderate pseudo strain hardening in tension, with tensile strain capacity typically on the order of 0.1% (Fig. 1).

From the viewpoint of production and processing feasibility, it is desirable if the multiple-cracking behavior can be achieved with lower fiber volume fractions up to about 2%, which makes it possible to use ordinary concrete mixing and casting equipment. To this end, Li [30] introduced a material design approach based on a systematic use of micromechanics and fracture mechanics-based criteria for multiple cracking. Materials developed using this concept are called *engineered cementitious composites* (ECC). Since materials of ECC class are central to the topic of this lecture, they will be discussed more specifically in the subsequent section.

More details on the history and nomenclature of fiber reinforced cementitious composites can be found for example in a recent review paper by Naaman [43] or JCI report [12].

1.2 Engineered cementitious composites

To achieve multiple cracking, a brittle-matrix fibrous composite has to satisfy two criteria formulated on the basis of fracture mechanics:

- The ‘steady state cracking criterion’ requires that a matrix crack can eventually grow under constant applied far field uniaxial tensile stress, as the bridging stress in the middle of the crack becomes equal to the applied stress. To that end, an appropriate balance between sufficiently high fiber bridging stress-transfer capacity and sufficiently low matrix toughness must exist.

- The ‘further cracking criterion’ requires that the matrix cracking strength (far field stress at which a throughout matrix crack forms) is lower than the maximum bridging stress (maximum stress that bridging fibers can transfer across the crack). Consequently, additional parallel cracks can form under further loading.

These criteria were set forth in works of Marshal and Cox [38], Cox et al. [6] and Naaman [41]. Employing micromechanics, Naaman [41] and Li and his co-workers, e.g. [33], [35], [25] expressed the conditions for multiple cracking and pseudo stain-hardening in terms of micromechanical parameters of fiber, matrix and fiber-matrix interface. These parameters included, for example, fiber volume fraction, fiber aspect ratio, fiber Young’s modulus, matrix Young’s modulus, matrix fracture toughness, initial flaw size, fiber-matrix bond characteristics, etc. Using these criteria, it was possible to optimize the material composition so as to achieve the desired multiple-cracking ability and overall ductility with a relatively small amount of short fibers. To emphasize the use of a rigorous micromechanics-based material design methodology, the materials are called *engineered cementitious composites* (ECCs) [30]. Although various fibers have been used in ECC (e.g. steel, high modulus polyethylene), nowadays a typical ECC consists of cementitious matrix with very fine aggregate and up to 2% by volume of polyvinyl alcohol (PVA) fibers 12 mm long and 40 μm in diameter. Such a composite exhibits overall tensile strain capacity up to several percent (Fig. 1), while maintaining crack width on the order of tens of μm [52].

It should be noticed in Figure 1 that, as opposed to UHPC, ECCs typically show moderate tensile strength but very high tensile strain capacity, which is associated with extensive and dense multiple cracking (Fig. 2b). This implies that structural use of the two types of strain-hardening composites should follow conceptually different ways. While structures with UHPC are basically designed not to crack, to make use of ECC features, multiple cracking must be accepted. Structural applications of ECC can be categorized into following groups:

1. Structural bearing elements, which have to sustain large deformations under alternating load, such as antiseismic coupling beams [40], walls [10] or short columns [11]. In these elements, ECC is used in conjunction with conventional reinforcement (reinforced ECC – R/ECC). In contrast to conventional R/C, ECC maintains overall integrity and interaction with reinforcing bars even at large deformations, which results in improved deformation and load carrying capacity under load reversals and enhanced ability to dissipate energy of the members.

2. Nonbearing elements or details which sustain moderate deformations in a harsh environment, such as waterway, dam or R/C bridge surface repair layers [48], ductile strips for elimination of shrinkage and temperature-induced cracking in bridge decks (link slab) [22], [36], or sewage lines. In these applications, the ability of ECC to accommodate inevitable deformations while maintaining submillimeter crack width is utilized to improve structural durability.

3. Highly strained structural details, where strain concentration occurs due to contact of materials with different stiffness, e.g. steel anchors in concrete [44].

The material cost of ECC is, in general, higher than that of conventional concrete and depends on the type of application. For example, in the case of the link slab, the cost of cast in-situ ECC was two to three times more expensive than concrete [22]. However, it should be noted that ECC is not intended to form the bulk of constructions; rather than that, it is strategically employed in elements where its superior properties can be fully utilized. Recent studies examining the environmental impact and lifecycle cost of ECC structures show that in a long time span, using ECC can lead to a considerable cost advantage and environmental benefits [26].

2. MULTISCALE FRAMEWORK FOR MODELING OF ECC MATERIALS

It follows from the discussion in the previous section that using novel materials, such as fiber reinforced cementitious composites, in engineering practice can bring about considerable advantages in terms of structural durability and safety. At the same time it poses many challenges, such as lack of empirical knowledge about the materials behavior and long-term performance, lack of established design provisions, and possibility or necessity to apply the new materials with unorthodox structural concepts and construction methods. To stand up to these challenges, it is desirable to employ innovative design methods.

So far, design of materials and design of structures have been mostly performed separately. Recently, however, the concept of *integrated structures and materials design* (ISMD) has been proposed by Li and Fischer [32], [31]. The integrated structures and materials design approach implies a two-way interaction between structural design and material development: structures are to be conceptually designed so as to take full advantage of materials’ properties, while materials are to be tailored to specific structural needs.

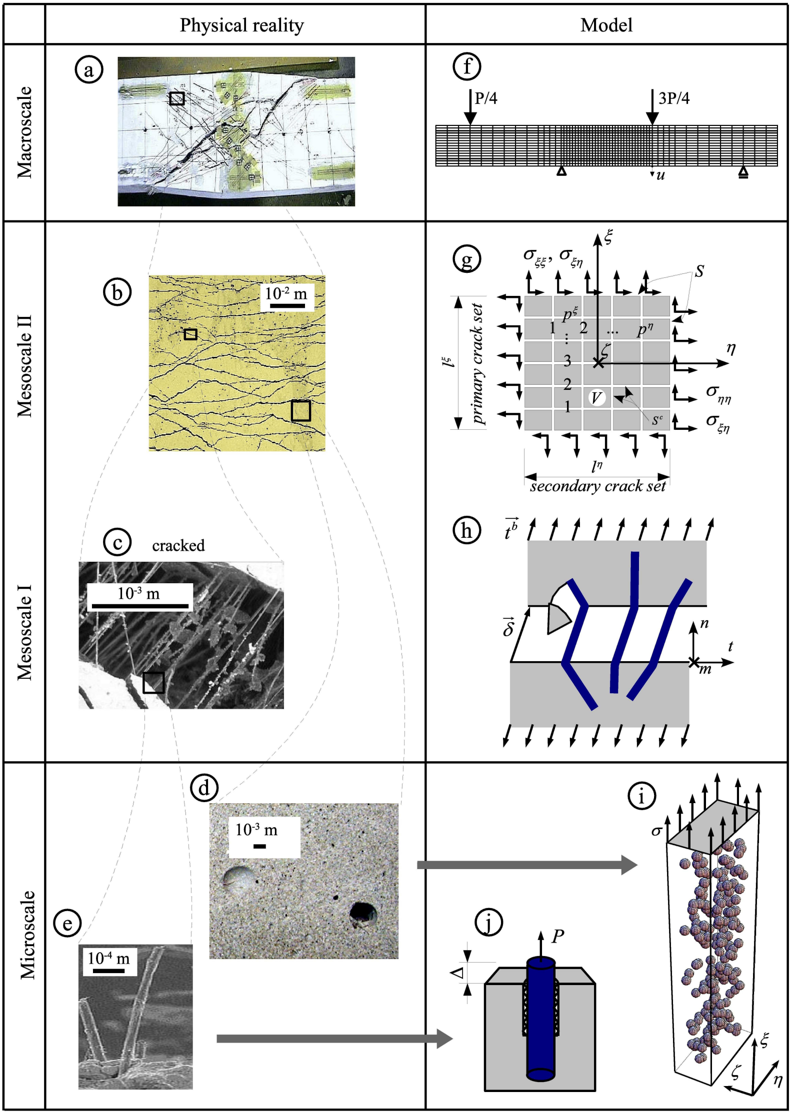

Figure 2 Relevant length scales in modeling of fracture in ECC [15]

For application of ISMD in engineering practice, it is necessary that suitable computational modeling tools are available. In particular, these tools must meet the following requirements:

- to allow reliable prediction of new materials' performance when they are used in structures;

- to provide insight into mechanisms of the materials nonlinear behavior and failure on structural scale;
- to provide a transparent linkage between the materials' composition/microstructure and their structural response.

Macroscopic material properties (such as strength) and behavior (such as hardening) that govern structural performance may be always attributed to physical phenomena that occur on a smaller length scale (such as propagation and localization of microdefects). When these sub-scale phenomena are looked at in detail, it possible to find that they result from mechanisms that occur on yet a finer length scale, and so on. Thus, it seems as natural that a modeling concept, which captures the dominant mechanisms across several length scales, should offer a reliable predictive capability of materials' macroscopic behavior while maintaining clear interconnection to their composition and microstructure.

In multiscale modeling, the goal is to predict the properties and behavior of complex materials or structures across all relevant length scales starting from fundamental physical mechanisms. Conceptually, two different approaches to multiscale modeling have been used. One of them attempts to employ simultaneously computational modules dealing with individual length scales, while communication between the modules is ensured by a sort of "handshaking" procedure [3]. Another type of multiscale concept employs a sequential hierarchy of analytical models, in which larger-scale models use coarse-grained representations of the material's substructure based on information obtained from more detailed, smaller-scale models.

Against this background, Kabele [15] set forth application of the sequential multiscale approach to modeling of structural performance of ECC materials. The main elements of this work are reiterated hereafter.

2.1 Relevant length scales

The requirements on structural performance in construction industry are usually specified on the scale of a structural member with dimensions on the order of 10^0 m. By structural performance we may understand, for example, load carrying capacity, ductility, or durability of a member. Very often, crack formation, propagation, and localization play the major role that affects the performance. While in the case of load and displacement capacity, the relationship to fracture is obvious, durability can be related to resistance against penetration of aggressive environmental agents, which in turn depends on a crack width. Accordingly, description of fracture phenomena should be central to our modeling effort.

The size of geometric details of structural members usually falls within the range of 10^{-1} to 10^{-2} m. At this length scale, which we will call a *macroscale*, it is possible to distinguish different materials of the member, such as ECC and conventional steel reinforcement as well as large localized cracks (macrocracks) – see Figure 2a. Phenomena like material strain-hardening and softening play the dominant role at this length scale.

Largest inhomogeneities in materials like ECC (fibers, initial defects, etc.) are distinguishable on a *microscale*, i.e. in the size range on the order of 10^{-3} to 10^{-6} m (Figs. 2d, e). Propagation of matrix cracks from preexisting defects and pullout of fibers that bridge these cracks can be considered as the dominant mechanisms at this length scale.

When an ECC material undergoes multiple cracking, the cracks form a dense pattern of sub-parallel surfaces with spacing on the order of 10^{-3} m and width on the order of 10^{-5} m, as obvious in Figure 2b. The figure also shows that a crack length reaches the order of magnitude of 10^{-2} m. The length scale at which we recognize these distributed multiple cracks will be denoted as *mesoscale II*. Evolution of the cracks' quantity as well as opening and sliding of these cracks are the phenomena that have the major effect at this length scale.

When a crack is looked at in detail, it is possible to see that it is bridged by a large number of fibers (Fig. 2c). The length scale that captures these numerous fibers bridging an individual crack will be referred to as a *mesoscale I*. Transfer of forces by fibers across a crack is the dominant mechanism on mesoscale I.

Within the scope of this paper, we will not look at details beyond the microscale. Mechanisms that take place on the length scale of pore structure and grains of cement paste as well as those that occur in the fiber-matrix interface transition zone (ITZ) will be treated phenomenologically.

2.2 Scales linking

In the sequential multiscale approach, a detailed analytical or numerical model is established for each of the relevant length scales – see Figures 2f-j and Section 2.3. In these models, only the dominant material substructures and associated mechanisms, which are recognizable at the corresponding length scale, are explicitly represented. To link the models across length scales, the following methods can be used.

2.2.1 Spatial averaging

The concept of spatial averaging is applicable only if it is possible to identify a spatial element, which contains numerous substructures (fibers, cracks, etc.) on a finer length scale, yet, on a larger scale, it is small enough that it can be viewed as a material point. Such an element is called a *representative volume element* (RVE). Then, it is acceptable and computationally convenient to model the material on the larger length scale by a spatially uniform constitutive law, which is determined as a relationship between an overall stress and overall deformation of the RVE. These overall quantities are defined as spatial averages of corresponding local quantities on the finer length scale, evaluated over the RVE. The relations among the local quantities, which are in general variable throughout the RVE, are expressed through the RVE's detailed analytical or numerical model.

In the hierarchy of the present multiscale model, the method of spatial averaging is applied to link the microscale and mesoscale I and to interconnect mesoscale I and mesoscale II. In the first case, a generalized bridging relationship on a single crack is obtained by averaging forces carried across the crack by a large number of fibers. In the second case, the RVE concept is employed to obtain effective properties of a material in a multiple cracking state while taking into account numerous cracks. These effective properties are then used when analyzing the behavior of a structural member on the macroscale. In special cases, when the entire structural member can be viewed as an RVE, the method of spatial averaging can be also utilized to interconnect the macroscale and the scale of a structural member.

2.2.2 Finite element method

Depending on the analyzed structural element size and loading conditions, during the transition from the mesoscale II or macroscale to the scale of a structural element it may not be possible to identify a representative volume element. In such cases, the scales are linked by the finite element method (FEM), in which appropriate constitutive and analytical models are implemented to represent the dominant phenomena at the lower scale.

2.3 Analytical models on individual length scales

2.3.1 Microscale – crack initiation

It has been generally accepted that formation of matrix cracks in fiber reinforced composites, when they are exposed to tension or shear, is associated with initial matrix flaws (e.g. [24], [51]). Some analytical models (e.g. [39], [35], [54]) idealize initial flaws as flat cracks bridged by fibers, while others consider them as round voids with small emanating "wing" cracks [20], which is more consistent with the observed microstructure (see Fig. 2d and [51]). The condition for propagation of these cracks is then formulated by comparing the stress intensity factor (or the energy release rate) due to applied load, possibly reduced by the effect of bridging, to the fracture resistance of matrix (fracture toughness K_m. or fracture energy J_m).

Note that the stress intensity factor or the energy release rate depends on the flaw shape, its size c and the applied load. Material at this length scale is then described by parameter K_m or J_m, the bridging traction, and flaw shape and size c. The latter can be given as a single value or by a statistical distribution.

By using the fracture criterion it is possible to estimate the first crack strength σ_{fc} (which is defined as the far-field stress at which the largest flaw initiates formation of the first matrix crack under uniform uniaxial tension) as well as cracking strengths associated with crack initiated at i-th flaw $^{(i)}\sigma_{cr}$.

Yet another approach is proposed by Dick-Nielsen et al. [7], who modeled the initial flaw as a traction-free slit and analyzed the stability of a cohesive crack propagating from it. The first crack strength, which they defined as the far-field stress at which the matrix crack propagation becomes unstable, matched well experimental values.

2.3.2 Microscale – fiber-matrix interaction

Cracks propagating through a composite intersect fibers. As these cracks open and/or slide, the fibers that bridge them are pulled out of a matrix. This results, first, in fiber debonding – propagation of a tunnel crack along the fiber-matrix interface from the crack surface toward the embedded end. The debonded part of the fiber stretches but its deformation is constrained by friction at the fiber-matrix interface. This process is modeled e.g. by Lin et al. [37] (Fig. 2j), who derived the relationship between fiber pullout force P and pullout displacement Δ for a short straight fiber perpendicular to the crack surface as:

$$P(\Delta)=\sqrt{\frac{\pi^2\tau_0 E_f d_f^3(1+\eta)}{2}\Delta+\frac{\pi^2 G_d E_f d_f^3(1+\eta)}{2}} \tag{1}$$

where $\eta = (E_f V_f)/(E_m V_m)$; V_m = matrix volume fraction; E_m = matrix elastic modulus, V_f = fiber volume fraction; E_f = fiber elastic modulus; d_f = fiber diameter; G_d = fiber-matrix chemical bond strength (fracture resistance against interface crack growth); and τ_0 = frictional stress on debonded interface (assumed constant due to small slip in this phase).

After a fiber has completely debonded, it starts to slip out of the matrix. Usually, the extension of the fiber is very small compared to the slip and therefore the fiber can be regarded as axially rigid in this phase. The slipping is resisted by the friction acting on the fiber-matrix interface. This friction can either increase or decrease with proceeding pullout, depending on the fiber material. For example, when synthetic PVA fibers are used, the shear-slip relation has a hardening character due to fiber abrasion and chips clogging the interface. For such a case, the P-Δ relationship is derived in [37] as:

$$P(\Delta) = \pi d_f \tau_0 \left[1 + \beta \frac{\Delta - \Delta_0}{d_f}\right](L_e - \Delta + \Delta_0) \tag{2}$$

where β = fiber-matrix interface slip-hardening parameter; L_e = fiber embedment length; and Δ_0 = pullout displacement at which debonding is completed (depends on η, E_f, d_f, G_d, τ_0, and L_e).

When a fiber is not perpendicular to the crack surface and/or it is pulled in direction inclined to the crack surface, it snubs against the matrix at the exit point. Li [29] uses the model of a frictional pulley to represent this effect. The pullout force is then expressed as:

$$P_\varphi(\Delta) = P(\Delta) e^{f\varphi} \tag{3}$$

where f = snubbing friction coefficient and φ = angle between the fiber embedment direction and the pullout direction (Fig. 3).

When a bridged crack undergoes opening and sliding, angle φ may vary between 0 and π. However, if a fiber is pulled backward (angle $\varphi \in \langle \pi/2, \pi \rangle$), it will almost certainly cause local damage (spalling) of the matrix at the exit point. A simple implementation of this phenomenon is proposed by Kabele in [14]: it is considered that spalling occurs for any fiber, which is pulled at angle exceeding a given critical value and the bridging effect of such a fiber is further neglected. The problem of matrix spalling is more precisely analyzed by Leung and Li [28], who derived the spalling criterion by a parametric study based on a detailed finite element analysis. An empirical formula for the spalling size is proposed by Yang et al. [56].

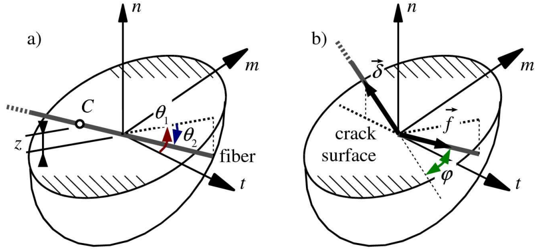

Figure 3 Fiber location and direction relative to crack surface: a) prior to pullout; b) after pullout due to crack opening and sliding [15]

2.3.3 Microscale – protruding fiber

When a fiber-bridged crack opens and slides, the pulled-out portions of fibers spanning the crack undergo deformation. To model this phenomenon, it is necessary to relate the vector of force transmitted by a fiber $\vec{P}=\{P_n, P_t, P_m\}$ to the vector of relative displacement of the fiber between crack faces $\vec{\delta}=\{\delta_n, \delta_t, \delta_m\}$ (see Fig. 4, Fig. 2h). Deformation in fiber axial direction is usually neglected, since its contribution is very small compared to the displacement due to debonding and pullout. On the other hand, resistance of the protruding fibers against relative tangential displacement of the crack faces (slip) may play a significant role.

One possible way to model this effect is based on considering the protruding part of a fiber as a beam, possibly supported by elastic-brittle foundation, and subjected to bending and shearing (e.g. [28], [27], [13], Fig. 4). The shear components of fiber force P_m, P_t then can be related to components of relative displacement $\vec{\delta}$, where δ_n corresponds to the beam span. Another approach consists in assuming that the protruding fiber is axially rigid, but perfectly flexible (i.e. that it transfers only axial force) – see e.g. [14]. It is then simple to treat finite displacements of the fiber by requiring the vector of relative displacements $\vec{\delta}$ and the fiber force vector $\vec{P}$ to be collinear. Which of the two approaches is appropriate depends on the fiber shear and axial stiffness and the ratio of the crack opening displacement δ_n and the fiber diameter d_f. In ECC with polymer fibers, when δ_n is comparable to d_f the fiber can be viewed as a beam, its bending can be neglected and the all tangential displacement can be attributed to shearing. On the other hand, when both δ_n, δ_m and δ_t are large compared to d_f, the assumption of perfectly flexible fiber is appropriate.

A bridging fiber may rupture before it is fully debonded or pulled out. Kanda and Li [23] report that synthetic PVA fibers tend to rupture at lower force than that corresponding to their nominal strength, when pulled in inclined direction from cementitious matrix. This phenomenon is attributed to abrasion of the fiber during pullout, snubbing, and extensive bending at

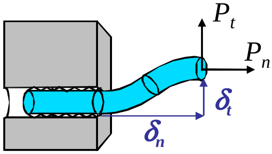

Figure 4 Bridging fiber force and relative displacement of crack surfaces

the exit point. In reference [23], the authors propose an empirical expression for the critical axial force at which fiber breaks.

2.3.4 Mesoscale I – fiber bridging

It is evident from Figure 2c, that on mesoscale I, an element of crack area can be modeled as a plane of discontinuity, which is bridged by a large number of fibers. Yet, as Figure 2b indicates, at the larger length scale (mesoscale II) the element appears as a point. Consequently, the element of crack area can be regarded as an RVE that collapsed form 3-D to 2-D (we refer to this RVE as $\mathrm{RVE}^{\mathrm{I}}$ to reflect association with mesoscale I). Overall behavior of $\mathrm{RVE}^{\mathrm{I}}$ is expressed as a relationship between bridging traction vector $\vec{t}^{\,b}$ and vector of relative displacement of the crack surfaces $\vec{\delta}$ (Fig. 2h).

In a material like ECC, location and direction of fibers can be assumed to be random within $\mathrm{RVE}^{\mathrm{I}}$. Behavior of individual fibers is described by the models discussed in Sections 2.3.2 and 2.3.3. The local quantities are the fiber forces and the fiber relative displacements. The position of a fiber relative to coordinate system *n-t-m* affixed to the crack surface can be expressed by angles θ_1 and θ_2 and perpendicular distance z between the fiber center C and the crack surface (Fig. 3a).

To obtain the relationship that describes the overall behavior of $\mathrm{RVE}^{\mathrm{I}}$, the element is exposed to uniform crack displacement $\vec{\delta}$ and corresponding traction $\vec{t}^{\,b}$ is calculated. The derivation of the $\vec{t}^{\,b}$ - $\vec{\delta}$ relationship is hereafter demonstrated for the case of perfectly flexible fibers following [14]. But the same concept is applicable, when protruding fibers are modeled as beams [13]. The derivation of fiber-bridging constitutive law is also reviewed and further elaborated in a recent publication by Yang et al. [56].

Assuming that fibers are perfectly flexible, each bridging fiber must exhibit the same pullout displacement $\Delta = \left|\vec{\delta}\right|$ (Figs. 3b and 2h). Furthermore, bridging force vectors of all fibers are parallel and collinear with vector $\vec{\delta}$. Then, following [34] and [14], the overall traction $\vec{t}^{\,b}$ can be expressed as a sum of forces contributed by all bridging fibers divided by the area of $\mathrm{RVE}^{\mathrm{I}}$. Thus, for a 3-D random fiber distribution and orientation, the magnitude of $\vec{t}^{\,b}$ is:

$$\left|\vec{t}^{\,b}\right| = \frac{V_f}{A_f} \int_{\theta_1=0}^{2\pi} \int_{\theta_2=0}^{\pi/2} \int_{\tilde{L}_e=0}^{1} P\left(\left|\vec{\delta}\right|, \tilde{L}_e\right) e^{f\varphi} \frac{\cos\theta_2}{2\pi} \sin\theta_2 \, d\tilde{L}_e \, d\theta_2 \, d\theta_1 \qquad (4)$$

where $\tilde{L}_e = \dfrac{L_e}{L_f/2}$ and L_f = fiber length. Either Equation 1 or Equation 2 is substituted for fiber force P, depending on the magnitude of fiber pullout displacement and fiber embedment length. Considering collinearity of vectors $\vec{\delta}$ and $\vec{t}^{\,b}$, we obtain the relationship that describes the overall behavior of $\mathrm{RVE}^{\mathrm{I}}$. Note that the effect of matrix spalling and fiber rupture can be incorporated in the preceding derivation by excluding affected fibers form contributing to the bridging traction [23], [14].

The concept outlined in the preceding paragraphs is also applicable to describe the behavior of a crack when it is unloaded. By unloading of a crack we understand the situation, when the absolute distance between crack surfaces closes, i.e. its incremental change is negative. Bridging fibers then do not undergo any further debonding and pullout. Instead, they elastically contract. When the fiber force becomes negative, the phenomena of fiber buckling and push-in into a matrix [55] as well as crack surfaces contact should be considered.

2.3.5 Mesoscale II – multiply-cracked material

Comparison of Figures 2 a, b shows that when a high performance composite undergoes multiple cracking, it may be possible to identify a spatial RVE that contains numerous cracks when viewed on mesoscale II, but it is small enough to be reduced into a material point on the macroscale. This RVE will be denoted as $\mathrm{RVE}^{\mathrm{II}}$ to indicate association with mesoscale II. The overall behavior of $\mathrm{RVE}^{\mathrm{II}}$ is then characterized by overall stress σ_{ij} and overall strain ε_{ij}, which are defined as volume averages of local stress and strain (respectively) over $\mathrm{RVE}^{\mathrm{II}}$. The relationship between σ_{ij} and ε_{ij} – the overall constitutive law – is obtained by exposing a model of $\mathrm{RVE}^{\mathrm{II}}$ that captures all details relevant to mesoscale II to a uniform stress along its boundaries and calculating its response in terms of overall strain.

2.3.5.1 Process of multiple cracking

While modeling the process of multiple cracking we consider the fracture phenomena, which are observed when a specimen of ECC material is exposed to uniform uniaxial stress σ in a direct tension test, as shown in Fig.2i. Then the whole specimen can be looked on as $\mathrm{RVE}^{\mathrm{II}}$. The process of multiple cracking is schematically depicted in Fig. 5 in terms of the applied stress σ and overall deformation ε. The specimen's behavior is initially linearly elastic until the applied load attains the level of the first crack strength σ_{fc}, at which a matrix crack starts to propagate from the largest preexisting flow. Due to low matrix toughness the crack propagates in an unstable manner through the specimen in the direction approximately

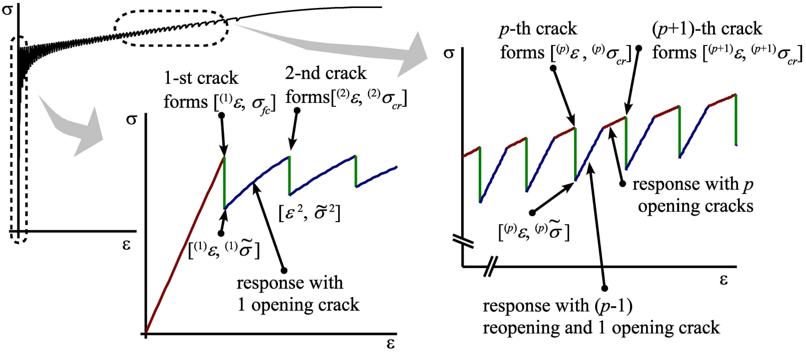

Figure 5 Process of multiple cracking under uniaxial tension [15]

perpendicular to the loading. However, the crack is bridged by fibers, which ensure that it maintains a flat shape with opening displacement almost uniform over its area. The crack exhibits a hardening response, i.e. increased load is needed for it to further open. It is noted that the flat shape of cracks and hardening crack response are direct consequences of satisfying the essential criteria for multiple cracking (Section 1.2). If additional loading is applied to the specimen, it causes opening of the existing crack and formation of another matrix crack from the next largest flaw. The whole scenario then repeats, resulting in a set of almost uniformly distributed cracks seen in Figure 2b. The process of multiple cracking terminates once the load carrying capacity of bridging is exhausted due to extensive fiber pullout, fiber rupture or matrix spalling on any of the crack planes. Consequently, bridging on this crack exhibits softening and fracture localizes into this crack.

If the sizes and spatial distribution of initial flaws are known or assumed, the criteria described in Section 2.3.1 can be used to determine the load level at which each flaw should develop into a throughout bridged crack. The bridging traction can be expressed using the mesoscale I model described in 2.3.4. When a throughout matrix crack forms, bridging fibers carry the entire acting load. This load is gradually transferred back to the intact composite adjacent to the crack through friction at the fiber-matrix interfaces. This implies that there exists a certain minimum distance between adjacent multiple cracks in which no new crack can form [53], [20]. Therefore, in some composites, saturation of multiple cracking can be observed, which is a state when all multiple cracks continue to open but no new crack forms.

2.3.5.2 Overall stress and strain

Consistently with the observations discussed in Section 2.3.5.1, RVE^{II} of a composite in the state of multiple cracking under uniform stress in 2-D, whose components develop in arbitrary non-proportional manner, is modeled with the following assumptions [14]:

- A set of multiple cracks starts to form when the magnitude of the maximum principal stress σ_1 attains the level of the first crack strength σ_{fc}. The cracks are planar within the RVE and are perpendicular to the maximum principal stress direction.
- Under further increase of stress, new cracks may form, but they are all assumed to be perpendicular to the principal stress direction determined when $\sigma_1 = \sigma_{fc}$. The number of cracks depends on the maximum level that crack-normal component of stress has attained throughout a history of loading/unloading. This relationship can be obtained using the procedure discussed in Section 2.3.5.1.
- All cracks may exhibit opening and sliding displacements, which are resisted by fiber bridging action. The bridging action is represented by the mesoscale I model described in Section 2.3.4.
- A secondary set of cracks may form, with cracks perpendicular to those of the primary set, if the normal stress in the secondary crack-normal direction exceeds the first crack strength. Other assumptions are the same as for the primary set. No interaction between the sets is assumed.

The model of RVE^{II} is shown in Figure 2g. Note that local Cartesian coordinate system ξ–η–ζ is introduced so that ξ–η plane corresponds to the loading plane and axis ξ is normal to the cracks of the primary set. This means that in the mesoscale I model, axes $m \equiv \zeta$, $n \equiv \xi$, $t \equiv \eta$ for the primary crack set or $m \equiv -\zeta$, $n \equiv \eta$, $t \equiv \xi$ for the secondary crack set.

We recall that to define the overall constitutive law, RVE^{II} is exposed to a uniform stress with components $\{\sigma_{\xi\xi}, \sigma_{\eta\eta}, \sigma_{\xi\eta}\}$ on its boundaries (Fig. 2g). As shown by Kabele [13], the overall stress is then equal to the applied stress. While analyzing the response of RVE^{II}, the state when matrix cracks unstably propagate from initial defects is neglected and only the state when they cut throughout the element is considered. Then the bridging tractions on each crack must be in equilibrium with the applied uniform stress.

The overall strain is expressed as:

$$\varepsilon_{ij} = \varepsilon_{ij}^{s} + \varepsilon_{ij}^{mc,\xi} + \varepsilon_{ij}^{mc,\eta} \tag{5}$$

where ε_{ij}^{s} = average strain in the continuous material between cracks and $\varepsilon_{ij}^{mc,\xi}$ and $\varepsilon_{ij}^{mc,\eta}$ (which we call cracking strains) represent the contribution to the total overall strain due to cracks of the primary and secondary set, respectively. The components of cracking strain can be expressed as [13]:

$$
\begin{aligned}
&\varepsilon_{\xi\xi}^{mc,\xi} = \frac{1}{V}\sum_{k=1}^{p^{\xi}} \int_{S_k^{\xi+}} {}^{(k)}\delta_{\xi}^{\xi} dS^{+},\ \varepsilon_{\eta\eta}^{mc,\xi} = 0,\ \varepsilon_{\xi\xi}^{mc,\eta} = 0,\ \varepsilon_{\eta\eta}^{mc,\eta} = \frac{1}{V}\sum_{k=1}^{p^{\eta}} \int_{S_k^{\eta+}} {}^{(k)}\delta_{\eta}^{\eta} dS^{+} \\
&\varepsilon_{\xi\eta}^{mc,\xi} = \varepsilon_{\eta\xi}^{mc,\xi} = \frac{1}{V}\sum_{k=1}^{p^{\xi}} \int_{S_k^{\xi+}} \frac{1}{2}\, {}^{(k)}\delta_{\eta}^{\xi} dS^{+},\ \varepsilon_{\xi\eta}^{mc,\eta} = \varepsilon_{\eta\xi}^{mc,\eta} = \frac{1}{V}\sum_{k=1}^{p^{\eta}} \int_{S_k^{\eta+}} \frac{1}{2}\, {}^{(k)}\delta_{\xi}^{\eta} dS^{+}
\end{aligned}
\tag{6}
$$

where δ_{ξ}^{ξ} and δ_{η}^{η} = opening displacements of cracks belonging to the primary and secondary set, respectively; δ_{ξ}^{ξ} and δ_{η}^{η} = crack sliding displacements; p^{ξ} and p^{η} = numbers of cracks in each set; and l^{ξ} and l^{η} = dimensions of RVE$^{\mathrm{II}}$ (see Fig. 2g).

We recall that the crack opening/sliding displacements as well as the number of cracks per length are related to the applied stress through the finer-scale models and that the overall strain ε_{ij}^{s} depends on the stress through an intact composite compliance. Thus, the overall constitutive relationship of RVE$^{\mathrm{II}}$ has been obtained.

2.3.6 Macroscale - structural member

The model on macroscale must capture geometrical details and distinct materials of structural members and possibly localized macrocracks, which occur in ECC after its hardening capacity is exhausted (Fig.2a). Behavior of the constituent materials is represented through their overall constitutive laws, such as that derived in Section 2.3.5. To analyze the overall response of the macroscale model, the method of spatial averaging may be used in special cases [14]. Otherwise, the FEM is employed.

2.4 Validation and application

In general, validation of the models for distinct length scales can be found in the literature referred to in each subsection of Section 2.3. The present concept of the multiscale modeling or its parts have been successfully used to solve various problems, such as simulation of damage evolution and failure in ECC under complex stress states [16], [5], simulation of the effect of flaw size distribution on uniaxial stress-strain relationship of ECC material [20], [15], and others. It has been also utilized in the material model of SHCC implemented in commercial FEM program ATENA [4].

3. MULTISCALE CHARACTERIZATION OF PVA-ECC EXPOSED TO AGGRESSIVE ENVIRONMENT

3.1 Introduction

As we discussed in Section 1.2, the use of ECC is often seen as one of possible ways to improve durability of concrete and R/C structures, especially of those exposed to harsh environment. From the durability point of view, it is important that the widths of the distributed multiple cracks remain in the sub-millimeter range, even when the overall strain attains the level of several percent. Since the overall mechanical behavior of ECC materials is closely related to their tailored microstructure, this ability can be estimated if the effects of aggressive environment on mechanical phenomena that take place at the micro- and mesoscale, are known. Kabele and his co-workers [17], [18], [19] recently experimentally investigate the effects of chloride environment and calcium-leaching environment on the mechanical behavior at various levels of the composites' microstructure. The two types of chemical attack were chosen so as to represent, in an accelerated manner, the typical environmental exposure anticipated in structures where ECC is used for improved durability, for example bridge decks, waterways, dams, retaining walls, sewers etc. Some results published in the most recent article [19] are reviewed hereafter.

3.2 Material

The material used for the present study was the ECC developed by Kajima Co. (Japan) [49], and produced by Futase Co. (Japan) under commercial name *ECC-crete*. The material is provided by the producer in the form of a dry mix. Its main constituents are Portland cement, fly ash, fine sand, and PVA fibers 40 μm in diameter and 12 mm long (2% by volume).

3.3 Specimen fabrication

The dry components, water and additives were mixed in a planetary mixer following a production manual [21]. The wet mix was cast into molds and covered with a plastic sheet. After hardening, specimens for tension, compression and fracture tests were prepared by cutting the cast pieces. Simultaneously with the cast pieces, samples for single-fiber pullout tests were prepared. These specimens were produced following the method explained in [17] and [18] by casting the mix without fibers into cylindrical molds (32 mm in diameter and 27 mm long) and embedding a single protruding fiber.

3.4 Accelerated ageing in aggressive environment

After hardening and cutting, the specimens were exposed to three types of environment. Samples denoted as O-series were kept in room conditions as a reference. Specimens of S-series were kept in conditions simulating in an accelerated manner environment of structures in proximity to sea or in areas where de-icing salts are used. The treatment consisted of 10 cycles of 5-days immersion in a saturated solution of NaCl at 20 ^{o}C and 2-days drying in oven at 50 ^{o}C. Samples of N-series were kept in calcium-leaching environment, which can be encountered, e.g., in waterways, dams, underground structures, sewers, or agricultural structures exposed to soft water or water containing nitrates. Leaching was preformed by immersing the samples for 70 days into 6 mol/l water solution of NH_4NO_3 at room temperature. After the chemical exposition, the specimens were left in room conditions for 18 to 32 days before being tested.

3.5 Testing methods

3.5.1 Three-point bending fracture tests

One of micromechanical parameters that play an important role in the energy-based criteria of multiple cracking (Section 1.2) is the crack-tip fracture energy J_{tip}. This quantity characterizes the resistance that a material offers against initiation of a matrix crack from a pre-existing flaw (perceived as a sharp crack) prior to activation of fiber bridging. For a composite with a small fiber volume fraction, it is approximately equal to the fracture energy of the unreinforced matrix J_m. In order to evaluate J_{tip}, three-point bending tests on notched beams were carried out. A typical specimen size was 10×20×150 mm, the notch length was 4-5 mm and the span was 140 mm. The tests were conducted under displacement control and the applied force, machine cross-head displacement and notch mouth opening displacement were recorded. Specimens' response was initially linear elastic. The onset of matrix fracture was clearly identifiable as sudden change in the slope of the load-deflection curves – the corresponding load was denoted as P_{cr}. Then we can use the linear elastic fracture mechanics to evaluate corresponding critical stress intensity factor $K_{I,tip}$ [50] as:

$$K_{I,tip} = \frac{6P_{cr}s}{4b^2t}\sqrt{\pi a}F\left(a,b\right) \tag{7}$$

where s = beam span, b = beam height, t = beam thickness, a = notch length, F = shape correction function [50]. The crack tip fracture energy is then calculated as:

$$J_{tip} = \frac{K_{I,tip}^2}{E} \tag{8}$$

where E composite Young modulus.

Considering that, due to their small size, most of the samples failed by a single crack, the three-point bending test was used to extract yet another characteristic, the fracture energy of a *single* fiber-bridged crack J_{tot}. This quantity is defined as energy released by formation of a unit area of a traction free crack. It involves the energy released by propagation of the matrix crack as well as a component due to disjoining the crack fiber-bridging. Since in ECC the latter far exceeds the former, J_{tot} actually characterizes the efficiency of fiber bridging. We evaluated J_{tot} by adapting the RILEM work-of-fracture method [46] (neglecting the beam self-weight) as:

$$J_{tot} = \frac{\int_{u=0}^{u_0} P\,du}{t(b-a)} \tag{9}$$

where P = applied force, u = load-point displacement, u_0 = displacement at complete separation.

3.5.2 Single fiber pullout tests

In order to gain a better understanding of the micromechanisms that govern the fiber bridging process, pullout tests were conducted on individual fibers, using the procedure described in [17] and [18]. To this end, mortar specimens with a single embedded fiber were used. The specimen was first fixed into a loading frame. Subsequently the protruding fiber was attached to a load cell fixed to the cross-head of the load machine. The test was conducted under displacement control. Applied force, cross-head displacement and protruding fiber-end displacement against the mortar body were recorded.

3.5.3 Uniaxial tension tests

Uniaxial tension tests were carried out to examine how the ECC overall tensile behavior is affected by the environmental exposure. The tests were conducted on prismatic specimens with typical dimensions of 10×20×150 mm. The specimens were strengthened by glued steel sheets on both ends so that the remaining free length was 70 mm. Each sample was attached to the loading machine by rigid grips and fitted with clip-on extensometer spanning the entire free length. Tests were conducted under displacement control and applied force, machine cross-head displacement and strain were recorded. From the processed stress vs. strain data, the following characteristics were identified: σ_{fc} = first cracking strength – stress at the point where the response exhibits the first drop in load or significant decrease of stiffness, σ_{pc} = post-cracking strength – maximum stress attained after first cracking, ε_{pc} = strain capacity – strain at σ_{pc}.

3.5.4 Uniaxial compression tests

The objective of uniaxial compression tests was to evaluate overall Young modulus and compressive strength of the composite. The tests were performed under displacement control on prismatic samples with typical dimensions of 12×12×70 mm.

3.6 Discussion of measured data

The averaged results of all valid test data are summarized in Table 1. The uniaxial compression tests revealed that the composite elastic modulus E was almost unaffected by the exposure to chloride and elevated temperature (S-series), while the compressive strength showed a slight reduction. On the other hand, nitrate environment (N-series), which is known to degrade cementitious materials by the process of calcium leaching, caused a drastic reduction of both of these values.

The average values of $K_{I,tip}$, J_{tip}, and J_{tot} calculated from notched beam fracture tests are listed in Table 1. It is seen that specimens of the S-series showed a significant increase in the resistance against initiation of matrix crack $K_{I,tip}$ when compared to the control specimens kept in room conditions (O-series). The same tendency is also observed when we calculate the corresponding crack tip fracture energy J_{tip}. Nitrate environment, on the other hand, caused reduction of the critical stress intensity factor $K_{I,tip}$. It is noteworthy, however, that the crack tip fracture energy J_{tip} actually exhibited increase for the N-series, which is attributed to the reduction of elastic modulus (see Eq. 8). The calculated fracture energy of a single crack J_{tot} decreased due to the action of chloride/drying environment. For the N-series, there was an apparent increase of J_{tot} (however, this might be due to the fact that multiple cracks developed in some specimens). It should be also noted that the fracture energy J_{tot} indeed exceeds the matrix fracture energy J_{tip} by 2 orders of magnitude, as it was discussed in section 3.5.1, and therefore can be interpreted as a measure of the fiber-bridging efficiency.

Figure 6 summarizes the valid results of individual fiber pullout tests in terms of applied force P_f and protruding fiber-end displacement Δ. As discussed in detail in [18], we can infer the micromechanical phenomena occurring during the fiber pullout process from these plots. Taking the upper curve of O-series in Figure 6 as an example, the distinct parts correspond to elastic deformation of the fiber before onset of debonding (initial linear part), debonding (hardening part), and pullout (descending part with rebounds). The sudden drop then corresponds to fiber rupture. The lower curve, on the contrary, indicates that the fiber did not rupture and was completely pulled out. The pull-out curves for S-series show a considerably different behavior. The debonding phase is much stiffer, indicating an increase in the chemical bond between fiber and matrix. The pullout phase, which follows the first load drop, shows a significant hardening, which is in all cases terminated by fiber rupture. This implies increased frictional bond and probably damage to the fiber surface. Specimens of the S-series sustained the highest loads on one hand, but brittle rupture on the other. In the case of N-series, the debonding resistance was considerably reduced. All fibers debonded at relatively low force and subsequently were pulled out without rupturing. The response was weak, but ductile.

It should be noticed that the results of the pullout tests are qualitatively consistent with the behavior on the scale of a single crack observed in the fracture tests. It can be concluded that the embrittlement associated with exposure to cycles of chloride and thermal treatment is due to the stronger fiber bond, which: a) results in the increase of force carried by bridging fibers and b) causes more damage to fiber surface during pullout. Both a) and b) then spur rupture of fiber bridging. On the contrary, leaching environment reduces the fiber bond, which facilitates fiber pullout and subsequently causes less brittle response of a fiber bridged crack.

Figure 7 shows the overall stress-strain curves obtained from the uniaxial tension tests. Averaged values of measured parameters are listed in Table 1. It is noted that the tests were performed on specimens with a relatively small cross section. In previous comparative tests it was found that this configuration, in general, results in lesser development of multiple cracks and lower tensile strain capacity than when larger specimens are used. In the present tests, the control specimens (O-series) exhibited moderate strain hardening and multiple cracking, with strain capacity ε_{pc} of about 0.6%. It should be noted that in most cases the hardening behavior

Table 1 Summary of experimental results of PVA-ECC [19]

Ser.	notched beam bending			uniaxial tension			uniaxial comp.	
	$K_{I,tip}$ (N.mm$^{-3/2}$)	J_{tip} (10^{-3} N/mm)	J_{tot} (N/mm)	σ_{fc} (MPa)	σ_{pc} (MPa)	ε_{pc} (%)	E (GPa)	strength (MPa)
O	13.4	6.65	2.06	3.68	3.47	0.62	27.8	54.6
S	17.3	10.7	1.72	5.83	4.11	0.26	28.0	48.2
N	11.0	12.0	3.48*)	1.81	2.62	2.25	10.1	23.7

*) multiple cracks developed in some specimens

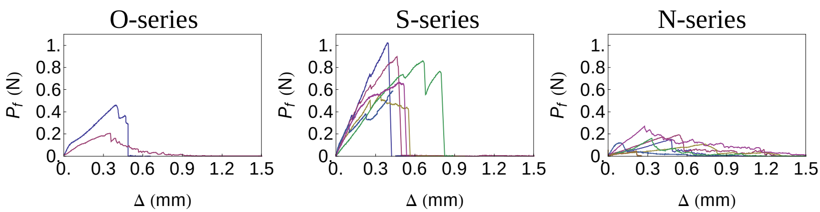

Figure 6 Results of single fiber pullout tests [19]

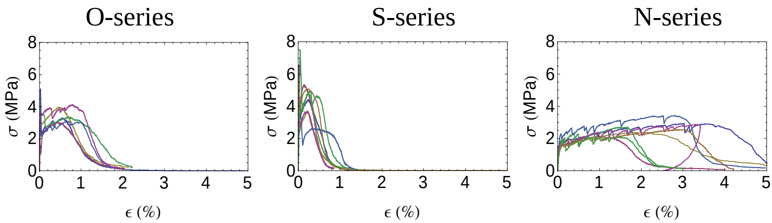

Figure 7 Results of uniaxial tension tests on PVA-ECC [19]

occurred after the load dropped following formation of the first matrix crack. The post-cracking strength σ_{pc} was lower than the first cracking strength σ_{fc}. Qualitatively similar behavior was observed for the S-series, though the first crack and post-cracking strength were higher and the overall ductility (ε_{pc}) was lower. Also, very few cracks developed in the specimens. On the contrary, the specimens of N-series showed a dense multiple cracking and high ductility of over 2%. This behavior was associated with a decrease of both first and post-cracking strengths, with the former becoming lower than the latter.

As it follows from Section 1.2, multiple cracking under uniform tension can be favorably affected by lowering the matrix cracking strength and increasing the fiber crack-bridging capacity. Considering that size of initial flaws (assumed as sharp cracks) is not affected by the environmental exposure, the first cracking strength is proportional to the critical stress intensity factor $K_{I,tip}$. Indeed, as we see in Table 1, $K_{I,tip}$ increased for S-series and decreased for N-series. By reviewing the values of J_{tot} in Table 1 one can see, that for S-series the efficiency of fiber bridging decreased while for N-series it increased. The results of uniaxial tension tests are thus again consistent with the behavior observed on lower scales.

4. CONCLUDING REMARKS AND FUTURE OUTLOOK

In this lecture, the author presented in a theoretically unified framework a hierarchy of interlinked analytical and numerical models that capture the fracture behavior of ECC materials across all relevant length scales, starting from the level of the composites' constituents and ending with the composites' performance when used in structural members. All of the models maintain a transparent connection to dominant mechanical phenomena that take place on the individual length scales. The system can be easily extended to account for phenomena like creep, fatigue, chemical degradation, etc. just by incorporating them on an appropriate scale.

In the second part of the lecture, the effects of aggressive environment on mechanical performance of PVA-ECC are studied from the perspective of the multiscale framework. The presented experimental results show that exposing PVA-ECC to cycles of immersion in chloride solution and drying at elevated temperature caused embrittlement of the composite, though it still retained some of the strain-hardening ability under uniaxial tension. Immersion in nitrate solution, on the other hand, caused reduction in strength but improvement of the strain-hardening behavior. These effects were observed consistently on different scales and linked to changes of micromechanical parameters, such as matrix toughness and fiber-matrix bond.

Although specific examples were not elaborated in this lecture, the presented modeling concept has been successfully used to solve various problems, such as simulation of the effect of flaw size distribution on uniaxial stress-strain relationship of ECC material [20], [15] or analysis of damage evolution and failure in ECC under complex stress states [16], [5]. It has been also employed for formulation of the material model for SHCC, which is implemented in the commercial FEM program ATENA [4]. Results of the present research have been utilized in the work of technical committee 208-HFC of RILEM [47] (esp. in subcommittee on structural design and performance and subcommittee on durability). The broad objective of this committee is to facilitate the transfer of the SHCC technology into engineering practice by proposing methodologies for structural design, material property characterization and field execution. The presented theoretical work has also served as a basis for further research, e.g. [8].

Strain hardening cementitious composites, such as ECC, have been presented as progressive materials with outstanding properties, which possess a potential to qualitatively improve performance of structures in terms of durability, reliability, and safety. Maintenance and construction of infrastructure is seen as a prime area for their future use. Along this line, an *International collaboration initiative to utilize SHCC for enhanced infrastructure durability*, which encompasses academic and industrial partners from the Americas, Europe, and Asia and in which the author is an active member, has been established in 2008. The initiative intends to develop integrated material technologies and structural concepts for efficient, environmentally friendly, durable, and sustainable infrastructure. Specifically, the technologies will aim at using locally available raw materials, green materials, natural fibers, low emission cement, etc. to achieve environmentally friendly strain hardening cementitious composites made from recyclable and renewable materials. The presented research is one of stepping stones for reaching these goals.

5. ACKNOWLEDGEMENTS

The research presented in this lecture has been carried out with financial support received by the author from the Contract of the Ministry of Education, Youth and Sports of the Czech Republic no. VZ 03 CEZ MSM 6840770003 and the Czech Science Foundation (grants no. 106/02/0678 and 103/05/0896). The author also thanks for collaboration to his research team, in particular his students Mr. Luděk Novák and Mr. Jaroslav Pekař.

6. REFERENCES

[1] Acker P, Behloul M. Ductal technology: a large spectrum of properties, a wide range of applications. In: Proc. of the International Symposium on Ultra High Performance Concrete. Kassel University Press, Kassel, Germany, 2004: 11-24.

[2] Brameshuber W. Textile Reinforced Concrete. State-of-the-Art Report of RILEM Technical Committee 201-TRC. RILEM Publications. 2006.

[3] Broughton JQ, Abraham FF, Bernstein N, Kaxiras E. Concurrent coupling of length scales: Methodology and application. Physical Review B. 1999; 60 (4): 2391-2403.

[4] Cervenka Consulting, Modelling fibre reinforced concrete in ATENA, http://www.cervenka.cz/papers. 2007.

[5] Cheung AKF, Leung CKY, Kabele P. Bond capacity of steel reinforcement in high performance fiber reinforced cementitious composites. Submitted to Fracture Mechanics of Concrete and Concrete Structures – FRAMCOS-7. 2009.

[6] Cox BN, Marshall DB, Thouless MD. Influence of statistical fiber strength distribution on matrix cracking in fiber composites. Acta Metallurgica. 1989; 37(7): 1933-1943.

[7] Dick-Nielsen L, Poulsen PN, Stang H, Olesen JF. Semi-analytical cohesive crack model for the analysis of first crack strength of mortar. In: Proceedings of the 17th Nordic Seminar on Computational Mechanics. 2004. p. 183-186.

[8] Dick-Nielsen L. Modeling of ECC Materials Using Numerical Formulations Based on Plasticity. Ph.D. Thesis. Technical University of Denmark, 2008.

[9] Farhat FA, Nicolaides D, Kanellopoulos A, Karihaloo BL. High performance fibre-reinforced cementitious composite (CARDIFRC) – Performance and application to retrofitting. Engineering Fracture Mechanics 2007; 74: 151-167.

[10] Fukuyama H, Suwada H, Mukai T. Test on high-performance wall elements with HPFRCC. In: Fischer G, Li VC, editors. Proceedings of International Workshop on High Performance Fiber Reinforced Cementitious Composites in Structural Applications. RILEM Publications. 2006. p. 365-374.
[11] Fukuyama H, Suwada H. Experimental response of HPFRCC dampers for structural control. Journal of Advanced Concrete Technology. 2003, 1(3): 317-326.
[12] JCI-DFRCC Committee. DFRCC terminology and application concepts, Journal of Advanced Concrete Technology. 2003; 1(3): 335-340.
[13] Kabele P. Equivalent continuum model of multiple cracking. Engineering Mechanics (Association for Engineering Mechanics, Czech Republic). 2002; 9 (1/2): 75-90.
[14] Kabele P. New developments in analytical modeling of mechanical behavior of ECCs. Journal of Advanced Concrete Technology. 2003; 1 (3): 253-264.
[15] Kabele P. Multiscale framework for modeling of fracture in high performance fiber reinforced cementitious composites. Engineering Fracture Mechanics. 2007; 74: 194-209.
[16] Kabele P, Kanakubo T. Experimental and numerical investigation of shear behavior of PVA-ECC in structural elements. In: Reinhardt HW, Naaman AE, editors. High Performance Fiber Reinforced Cementitious Composites (HPFRCC5). RILEM Publications. 2007, p. 137-145.
[17] Kabele P, Němeček J, Novák L, Kopecký L. Effects of calcium leaching on interfacial properties of PVA fibers in cementitious matrix. Engineering Mechanics. 2006; 13(4): 285-296.
[18] Kabele P, Novák L, Němeček J, Kopecký L. Effects of chemical exposure on bond between synthetic fiber and cementitious matrix. In: Hegger J, Brameshuber W, Will N. Textile Reinforced Concrete - Proc. of the 1st International RILEM Conference. RILEM Publications. 2006. p. 91-99.
[19] Kabele P, Pekař J. Multiscale experimental investigation of PVA-ECC exposed to aggressive environment. Accepted for publication in 4th International Conference on Construction Materials: Performance, Innovations and Structural Implications, ConMat’09, Nagoya, Japan. 2009.
[20] Kabele P, Stemberk M. Stochastic model of multiple cracking process in fiber reinforced cementitious composites. In: Proc. of International Conference on Fracture ICF XI, Turin, Italy, 20.-25.3.2005. (CD-ROM).
[21] Kajima Technical Research Institute. Mixing Manual of ECC Dry-Mix for Casting, KaTRI, Japan. 2006.
[22] Kalousdian A. ECC replaces bridge joints. Michigan Contractor and Builder. March 18 2006.
[23] Kanda T, Li VC. Effect of fiber strength and fiber-matrix interface on crack bridging in cement composites. ASCE J. of Engineering Mechanics. 1999; 125 (3): 290-299.
[24] Kanda T, Li VC. Multiple cracking sequence and saturation in fiber reinforced cementitious composites. Concrete Research and Technology, JCI. 1998; 9 (2): 19-33.

[25] Kanda T, Li VC. Practical design criteria for saturated pseudo strain hardening behavior in ECC. Journal of Advanced Concrete Technology. 2006; 4(1): 59-72.
[26] Lepech M. New infrastructure materials, structures, and management techniques in global climate change mitigation. Invited lecture at DTU BYG, Lyngby, Denmark, November 24, 2008.
[27] Leung CKY, Chi J. Crack bridging force in random ductile fiber brittle matrix composites. Journal of Engineering Mechanics. 1995; 121 (12): 1315-1323.
[28] Leung CKY, Li VC. Effect of fiber inclination on crack bridging stress in brittle fiber reinforced brittle matrix composites. Journal of Mechanics and Physics of Solids. 1992; 40 (6): 1333-1362.
[29] Li VC. Post-crack scaling relations for fiber-reinforced cementitious composites. ASCE Journal of Materials in Civil Engineering. 1992; 4 (1): 41-57.
[30] Li VC. On Engineered Cementitious Composites (ECC) – A review of the material and its applications. Journal of Advanced Concrete Technology. 2003; 1(3): 215-230.
[31] Li VC. Integrated materials and structures design. Materials and Structures. 2007; 40(4): 387-396.
[32] Li VC, Fischer G. Reinforced ECC – an evolution from materials to structures. In: Proc. of the First FIB Congress. 2002. p. 105-122.
[33] Li VC, Leung CKY. Steady state and multiple cracking of short random fiber composites. ASCE Journal of Engineering Mechanics. 1992; 188 (11): 2246-2264.
[34] Li VC, Wang Y, Backer S. A micromechanical model of tension-softening and bridging toughening of short random fiber reinforced brittle matrix composites. Journal of Mechanics and Physics of Solids. 1991; 39 (5): 607-625.
[35] Li VC, Wu HC. Conditions for pseudo strain-hardening in fiber reinforced brittle matrix composites. Journal of Applied Mechanics Review. 1992; 45 (8): 390-398.
[36] Li VC, Zhang J. A ductile strip used for eliminating shrinkage and temperature cracks in concrete pavements and bridge decks. US Patent No. 6,694,690, Issued on Feb. 24, 2004.
[37] Lin Z, Kanda T, Li VC. On interface characterization and performance of fiber-reinforced cementitious composites. Concrete Science and Engineering. 1999; 1: 173-184.
[38] Marshall DB, Cox BN A J-integral method for calculating steady-state matrix cracking stresses in composites, Mechanics of Materials. 1988; 7(2): 127-133.
[39] Marshall DB, Cox BN, Evans AG. The mechanics of matrix cracking in brittle-matrix fiber composites. Acta Metallurgica 1985; 33(11): 2013-2021.
[40] Maruta M, Kanda T, Nagai S, Yamamoto Y. New high-rise RC structure using pre-cast ECC coupling beam. Concrete Journal. 2005. 43(11): 18-26 (in Japanese).
[41] Naaman AE. High performance fiber reinforced cement composites. In: Concrete Structures for the Future, Proc. of IABSE Symposium, Paris, France. 1987: 371-376.

[42] Naaman AE. SIFCON: tailored properties for structural performance. In: Reinhardt HW, Naaman AE, editors. High Performance Fiber Reinforced Cement Composites. 1992. p. 18-38.
[43] Naaman AE. Tensile strain-hardening FRC composites: Historical evolution since the 1960. In: Grosse U, editor. Advances in Construction Materials. Springer. Berlin Heidelberg. 2007. p. 181-202.
[44] Qian S, Li VC. Influence of concrete material ductility on headed anchor performance. ACI Materials Journal. 2009; 106(1): 72-81.
[45] Reinhardt HW, Naaman AE, co-editors. High Performance Fiber Reinforced Cement Composites. RILEM Publications. 1992.
[46] RILEM TC-50 FMC. Determination of the fracture energy of mortar and concrete by means of three-point bend tests on notched beams. Materials and Structures. 1985; 18(4): 287-290.
[47] RILEM, Technical Committee 208-HFC. http://www.rilem.net/technicalCommittees.php. 2004.
[48] Rokugo K, Kunieda M, Miyazato S. Structural applications of HPFRCC in Japan. In: M.S. Konsta-Gdoutos, editor. Measuring, Monitoring and Modeling Concrete Properties. Springer. 2006. p. 17–23.
[49] Sakata N, Suda, K, Kanda T, Fukuda I, Hiraishi T, Tomoe S. Development on Engineered Cementitious Composite. KaTRI Annual Report, 2004; 52: 233-238 (in Japanese).
[50] Tada H, Paris PC, Irwin GR. The Stress Analysis of Cracks Handbook. ASME. 2000: 58-60.
[51] Wang S, Li VC. Tailoring of pre-existing flaws in ECC matrix for saturated strain hardening. In: Li VC, Leung CKY, Willam KJ, Billington SL, editors. Fracture Mechanics of Concrete Structures 5. 2004. p. 1005-1012.
[52] Wang S, Li VC. Polyvinyl alcohol fiber reinforced engineered cementitious composites: material design and performances. In: Fischer G, Li VC, editors. Proceedings of International Workshop on High Performance Fiber Reinforced Cementitious Composites in Structural Applications. RILEM Publications. 2006. p. 65-73.
[53] Wu HC, Li VC. Snubbing and bundling effects on multiple crack spacing of discontinuous random fiber-reinforced brittle matrix composites. Journal of American Ceramic Society. 1992; 75 (12): 3487-3489.
[54] Wu HC, Li VC. Stochastic process of multiple cracking in discontinuous random fiber reinforced brittle matrix composites. International Journal of Damage Mechanics. 1995; 4: 83-102.
[55] Wu HC, Matsumoto T, Li VC. Buckling of bridging fibers in composites. Journal of Materials Science Letters. 1994; 13: 1800-1803.
[56] Yang E-H, Wang S, Yang Y, Li VC. Fiber-bridging constitutive law of Engineered Cementitious Composites. Journal of Advanced Concrete Technology. 2008; 6(1): 181-193.

Doc. Ing. Petr Kabele, Ph.D.

Curriculum Vitae

Date of birth (day/month/year)**:** 03/05/1968
Place of birth: Prague, Czech Republic
Nationality: Czech
Work address:
Department of Mechanics, Faculty of Civil Engineering
Czech Technical University in Prague
Thákurova 7, CZ-166 29 Praha 6, Czech Republic
tel: +420-2435 4485
e-mail: petr.kabele@fsv.cvut.cz

Educational background

7/1986 – 9/1990:	undergraduate study, Faculty of Civil Engineering CTU in Prague (Thákurova 7, Praha 6, Czech Republic)
10/1990 – 9/1992:	Master's study, Graduate School, Department of Civil Engineering, University of Tokyo (Hongo 7-3-1, Bunkyo-ku, Tokyo, Japan)
9/1992:	degree M.Eng. – Master of Engineering (Civil Engineering), diploma thesis: „Analysis of Concrete Structures by FEM-BEM Superposition Method“
5/1994:	degree M.Eng. officially recognized by CTU in Prague as „inženýr (Ing.)“
10/1992 – 9/1995:	doctoral study, Graduate School, Department of Civil Engineering, University of Tokyo
9/1995:	degree Ph.D. – Doctor of Philosophy (Civil Engineering), dissertation: „Analytical Modeling and Fracture Analysis of Engineered Cementitious Composites“
5/2001:	academic title doc. – docent, habilitation in the field of Theory of building structures and materials, Faculty of Civil Engineering CTU in Prague, habilitation thesis: „Assessment of Structural Performance of Engineered Cementitious Composites by Computer Simulation“

Professional experience

10/1995 – 3/1996:	Research Associate Department of Civil Engineering, University of Tokyo
4/1996 – 5/1998:	Assistant Professor Department of Civil Engineering, University of Tokyo
6/1998 – 3/1999:	Associate Professor

	Department of Civil Engineering, University of Tokyo
6/1999 – 6/2001:	Assistant Professor Faculty of Civil Engineering CTU in Prague, Department of Structural Mechanics
7/2001 – present:	Associate Professor Faculty of Civil Engineering CTU in Prague, Department of Mechanics

Main scientific interests

- analytical and numerical modeling of nonlinear behavior of materials (esp. cement-based composites),
- multiscale approaches in modeling and experimental testing of materials (esp. in aggressive environment, at high temperatures),
- application of numerical methods for simulations of complex problems (building demolition, geological processes, nanoindentation),
- continuum mechanics, fracture mechanics, numerical mechanics, micromechanics.

Professional and scientific activities

- author and co-author of over 60 professional publications, of which 11 are articles in international impact or refereed journals, over 35 are articles in international conferences
- 25 citations in SCI-EXP, CPCI-S, SCOPUS (excluding self-citations)
- principal investigator of 5 grants (GAČR 103/02/0658, GAČR 106/02/0678, GAČR 103/05/0896, RP MŠMT 13.8, RP MŠMT 17), co-investigator GAČR 103/07/1660
- collaboration on 3 international grants, 8 Czech grants and supervisor of 3 Ph.D. grants CTU
- member/advisor of 3 professional committees
    - Japan Concrete Institute, Task Committee on High Performance Fiber Reinforced Cementitious Composites (HPFRCC), 2001-2004 (international board member)
    - Japan Society of Civil Engineers, Sub-Committee 334, Recommendations for Design and Construction of HPFRCC, 2004-2006 (advisor)
    - RILEM, Technical Committee 208-HFC High Performance Fibre Reinforced Cementitious Composites, 2004-2009 (active member)
- member of scientific board of 5 international conferences
- member of evaluation board for applicants for the scholarship of Japanese Ministry of Education (Monbukagakusho) at the Embassy of Japan in the CR

- reviewer of 14 international professional journals
- member of RILEM and Japan Society of Civil Engineers
- supervised and co-supervised 9 Ph.D., 6 Master’s and 4 Bachelor’s theses
- language skills: English (fluent), Japanese (fluent spoken), Czech (native)

Selected journal publications from the past 10 years

Article in journal with impact factor

Kabele, P. - Yamaguchi, E. - Horii, H.: FEM-BEM Superposition Method for Fracture Analysis of Quasi-brittle Structures. International Journal of Fracture. 1999, vol. 100, no. 3, p. 249-274. ISSN 0376-9429. *IF: 1.003. WoS citations excl. self-citations: 2*

Li, VC - Horii, H - Kabele, P. - Kanda, T - Lim, YM: Repair and Retrofit with Engineered Cementitious Composites. Engineering Fracture Mechanics. 2000, vol. 65, no. 2-3, p. 317-334. ISSN 0013-7944. *IF: 1.227. WoS citations excl. self-citations: 7*

Kabele, P.: Multiscale Framework for Modeling of Fracture in High Performance Fiber Reinforced Cementitious Composites. Engineering Fracture Mechanics. 2007, vol. 74, no. 1-2, p. 194-209. ISSN 0013-7944. IF: 1.227. *WoS citations excl. self-citations: 0*

Žák, J. - Vyhnálek, B. - Kabele, P.: Is there a Relationship between Magmatic Fabrics and Brittle Fractures in Plutons? A View Based on Structural Analysis, Anisotropy of Magnetic Susceptibility and Thermo-mechanical Modelling of the Tanvald Pluton (Bohemian Massif). Physics of the Earth and Planetary Interiors. 2006, vol. 157, no. 3-4, p. 286-310. ISSN 0031-9201. *IF: 2.026. WoS citations excl. self-citations: 1*

Žák, J. - Paterson, S.R. - Janoušek, V. - Kabele, P.: The Mammoth Peak Sheeted Complex, Tuolumne Batholith, Sierra Nevada, California: a Record of Initial Growth or Late Thermal Contraction in a Magma Chamber? Contributions to Mineralogy and Petrology, published online 13 March 2009, 24 p. ISSN: 0010-7999. *IF: 3.216: WoS citations excl. self-citations: 0*

Article in international refereed journal

Kabele, P.: Equivalent Continuum Model of Multiple Cracking. Engineering Mechanics. 2002, vol. 9, no. 1/2, p. 75-90. ISSN 1802-1484. *WoS citations excl. self-citations: 0*

Kabele, P.: New Developments in Analytical Modeling of Mechanical Behavior of ECC. Journal of Advanced Concrete Technology. 2003, vol. 1, no. 3, p. 253-264. ISSN 1346-8014. *WoS citations excl. self-citations: 0*

Kabele, P. - Němeček, J. - Novák, L. - Kopecký, L.: Effects of Calcium Leaching on Interfacial Properties of PVA Fibers in Cementitious Matrix. Engineering Mechanics. 2006, vol. 13, no. 4, p. 285-296. ISSN 1802-1484. *WoS citations excl. self-citations: 0*